

Calculation of Temperature-Dependent Hadronic Correlation Functions of Pseudoscalar and Vector Currents

Bing He, Hu Li, C. M. Shakin,* and Qing Sun

Department of Physics and Center for Nuclear Theory

Brooklyn College of the City University of New York

Brooklyn, New York 11210

(Dated: December, 2002)

Abstract

We make use of the Nambu-Jona-Lasinio (NJL) formalism and real-time finite-temperature field theory to calculate hadronic current correlation functions in the deconfined phase of quantum chromodynamics (QCD). We consider both pseudoscalar and vector currents and compare our results with those obtained in lattice simulations of QCD. Our results are similar to those obtained in the lattice simulations for $T = 1.5 T_c$, where T_c is the temperature of the confinement-deconfinement transition. For $T = 3.0 T_c$ our results do not exhibit the resonances obtained from the lattice simulations. However, the errors presented for the lattice results are large and it is possible that our results at $T = 3.0 T_c$ are consistent with the lattice results when these errors are taken into account. Since the method used in the lattice analysis to obtain the spectral functions requires assumptions about the likelihood of a particular form for the spectral function, we believe our calculations will be useful to researchers who wish to calculate hadronic current correlation functions at finite temperature using lattice-based methods. Our model makes use of temperature-dependent coupling constants for the NJL model. We present an argument that such temperature dependence is necessary, if the results of the model are to be consistent with what is known concerning QCD thermodynamics.

PACS numbers: 12.39.Fe, 12.38.Aw, 14.65.Bt

*email:casbc@cunyvm.cuny.edu

I. INTRODUCTION

In recent years we have seen a great deal of interest in the properties of dense matter, with particular attention given to diquark condensation and color superconductivity [1]. Since it is difficult to study the properties of dense matters in lattice simulations of QCD [2], the Nambu-Jona-Lasinio (NJL) model and closely related instanton-based models have been used in such studies. We have become interested in a possible density dependence of the coupling constants of chiral Lagrangian models, since density dependence of the coupling parameters could affect the conclusions drawn from the studies of dense matter. We have introduced density-dependent coupling constants for the NJL model in earlier works [3, 4], and have presented some arguments that such density dependence may be necessary [4]. However, it is much easier to discuss the temperature dependence of NJL coupling parameters, rather than the density dependence, since a good deal is known concerning finite-temperature QCD thermodynamics [5]. In particular, the study of a gluon gas at high temperature suggests that the system is well described as weakly interacting for $T \gtrsim 6T_c$, where T_c is the temperature of the confinement-deconfinement phase transition. (See Fig. 1.3 of Ref. [5].)

In this work we suggest that rather straightforward calculations of hadronic current correlation functions at finite temperature can provide information concerning a possible temperature dependence of the NJL coupling parameters. We perform calculations of hadronic current correlation functions for pseudoscalar and vector currents in the range $1.2 \leq T/T_c \leq 5.88$. We make use of two models for the temperature dependence of the NJL coupling parameters. For model 1, we use $G(T) = G[1 - 0.17(T/T_c)]$, which was the form used in our previous studies of meson properties [6] and hadronic current correlation functions [7] at finite temperature. In this work we also introduce a model 2, for which $G(T) = G[1 - 0.0289(T/T_c)^2]$. In both cases, $G(T) = 0$ for $T/T_c = 5.88$. For values of $T/T_c > 5.88$ we put $G(T) = 0$ for both models.

For the sake of completeness we present the Lagrangian of a generalized NJL model that

we have used in our studies of meson properties at finite temperature and density

$$\begin{aligned}
\mathcal{L} = & \bar{q}(i\partial - m^0)q + \frac{G_S}{2} \sum_{i=0}^8 [(\bar{q}\lambda^i q)^2 + (\bar{q}i\gamma_5\lambda^i q)^2] \\
& - \frac{G_V}{2} \sum_{i=0}^8 [(\bar{q}\lambda^i\gamma_\mu q)^2 + (\bar{q}\lambda^i\gamma_5\gamma_\mu q)^2] \\
& + \frac{G_D}{2} \{ \det[\bar{q}(1 + \gamma_5)q] + \det[\bar{q}(1 - \gamma_5)q] \} \\
& + \mathcal{L}_{conf}.
\end{aligned} \tag{1.1}$$

Here, m^0 is a current quark mass matrix, $m^0 = \text{diag}(m_u^0, m_d^0, m_s^0)$. The λ^i are the Gell-Mann (flavor) matrices. Here, $\lambda^0 = \sqrt{2/3} \mathbf{1}$ with $\mathbf{1}$ being the unit matrix. The fourth term on the right-hand side of Eq. (1.1) is the 't Hooft interaction. Finally, \mathcal{L}_{conf} represents the model of confinement we have used in our work.

We have recently reported results of our calculations of the temperature dependence of the spectra of various mesons [6]. These calculations were made using our generalized NJL model which includes a covariant model of confinement. We have presented results for the π , K , a_0 , f_0 and K_0^* mesons in Ref. [6]. In that work, temperature-dependent constituent quark masses were calculated using the equation [8]

$$m(T) = m^0 + 2G_S(T)N_c \frac{m(T)}{\pi^2} \int_0^\Lambda dp \frac{p^2}{E_p} \tanh\left(\frac{1}{2}\beta E_p\right). \tag{1.2}$$

Here, m^0 is the current quark mass, $G_S(T)$ is a temperature-dependent coupling constant introduced in our model. (In Ref [6] we used model 1 for $G_S(T)$.) Here, $N_c = 3$ is the number of colors, $\beta = 1/T$ and $E_p = [\vec{p}^2 + m^2(T)]^{1/2}$. Further, $\Lambda = 0.631$ GeV is a cutoff such that $|\vec{p}| \leq \Lambda$. Results obtained for the up (or down) and strange quark masses are given in Fig. 1. In calculating the constituent mass values we have neglected the confining interaction. That interaction was taken into account in our earlier Euclidean-space calculation of the quark self-energy [9], which also included the effects related to the 't Hooft interaction. We found that, to a good approximation, we could neglect the confining and 't Hooft interactions, if we modified the value of the NJL coupling constant, G_S , and we adopt that approach when using Eq. (1.2).

The organization of our work is as follows. In Sec. II we review our calculations of polarization functions at finite temperature. In Sec. III we discuss the calculation of hadronic current correlation functions, making use of the results presented in Sec. II. In Sec. IV and V

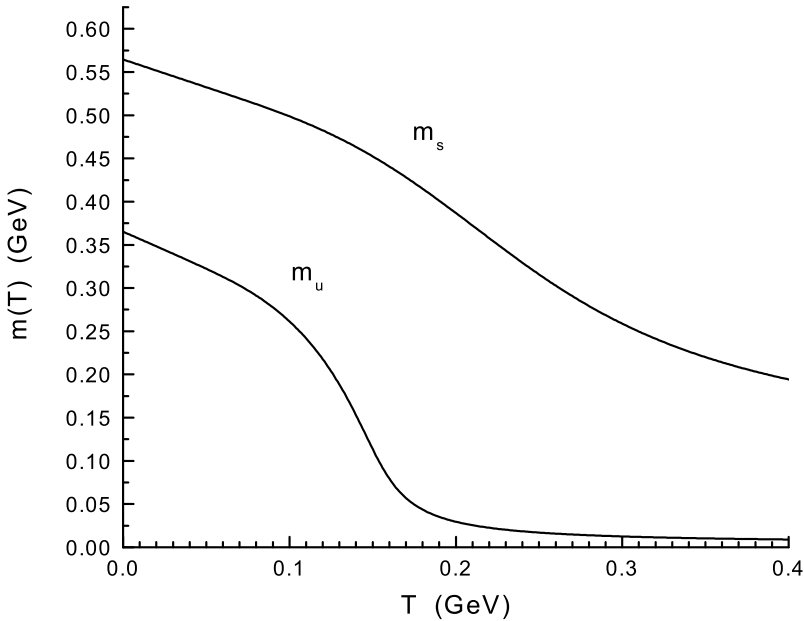


FIG. 1: Temperature dependent constituent mass values, $m_u(T)$ and $m_s(T)$, calculated in a mean field approximation [8] are shown. [See Eq. (1.2)]. Here $m_u^0 = 0.0055$ GeV, $m_s^0 = 0.120$ GeV, and $G(T) = 5.691[1 - 0.17(T/T_c)]$, if we use Klevansky's notation [8]. (The value of G_S of Eq. (1.1) is twice the value of G used in Ref. [8]).

we present the results of our numerical calculations of correlators of pseudoscalar and vector currents, respectively. We also compare our results to some recent lattice calculations of pseudoscalar and vector correlators [10-12]. Finally, in Sec. VI we present same further discussion and conclusions.

II. POLARIZATION FUNCTIONS AT FINITE TEMPERATURE

The basic polarization function that is calculated in the NJL model is shown in Fig. 2. We will consider calculations of such functions in the frame where $\vec{P} = 0$. In our earlier work, calculations were made after a confinement vertex was included. That vertex is represented by the filled triangular region in Fig. 2. However, we here consider calculations for $T \geq 1.2 T_c$ where confinement may be neglected. We will, however, use the temperature-dependent mass values shown in Fig. 1.

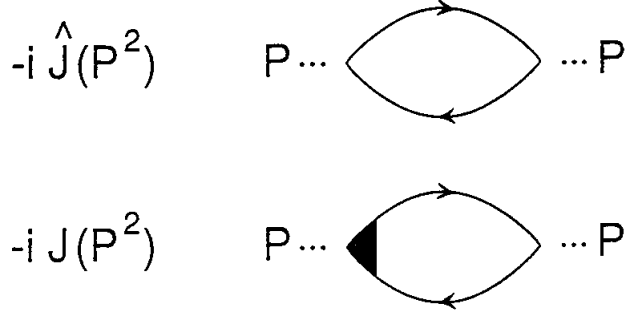


FIG. 2: The upper figure represents the basic polarization diagram of the NJL model in which the lines represent a constituent quark and a constituent antiquark. The lower figure shows a confinement vertex [filled triangular region] used in our earlier work. For the present work we neglect confinement for $T \geq 1.2 T_c$, with $T_c = 150$ MeV.

The procedure we adopt is based upon the real-time finite-temperature formalism, in which the imaginary part of the polarization function may be calculated. Then, the real part of the function is obtained using a dispersion relation. The result we need for this work has been already given in the work of Kobes and Semenoff [13]. (In Ref. [13] the quark momentum in Fig. 2 is k and the antiquark momentum is $k - P$. We will adopt that notation in this section for ease of reference to the results presented in Ref. [13].) With reference to Eq. (5.4) of Ref. [13], we write the imaginary part of the scalar polarization function as

$$\begin{aligned} \text{Im } J_S(P^2, T) = & \frac{1}{2} (2N_c) \beta_S \epsilon(P^0) \int \frac{d^3k}{(2\pi)^3} e^{-\vec{k}^2/\alpha^2} \left(\frac{2\pi}{2E_1(k)2E_2(k)} \right) \\ & \{(1 - n_1(k) - n_2(k))\delta(P^0 - E_1(k) - E_2(k)) \\ & \quad - (n_1(k) - n_2(k))\delta(P^0 + E_1(k) - E_2(k)) \\ & \quad - (n_2(k) - n_1(k))\delta(P^0 - E_1(k) + E_2(k)) \\ & \quad - (1 - n_1(k) - n_2(k))\delta(P^0 + E_1(k) + E_2(k))\} . \end{aligned} \quad (2.1)$$

Here, $E_1(k) = [\vec{k}^2 + m_1^2(T)]^{1/2}$. Relative to Eq. (5.4) of Ref. [13], we have changed the sign, removed a factor of g^2 and have included a statistical factor of $2N_c$, where the factor of 2 arises from the flavor trace. In addition, we have included a Gaussian regulator, $\exp[-\vec{k}^2/\alpha^2]$, with $\alpha = 0.605$ GeV, which is the same as that used in most of our applications

of the NJL model in the calculation of meson properties. We also note that

$$n_1(k) = \frac{1}{e^{\beta E_1(k)} + 1}, \quad (2.2)$$

and

$$n_2(k) = \frac{1}{e^{\beta E_2(k)} + 1}. \quad (2.3)$$

For the calculation of the imaginary part of the polarization function, we may put $k^2 = m_1^2(T)$ and $(k - P)^2 = m_2^2(T)$, since in that calculation the quark and antiquark are on-mass-shell. In Eq. (2.1) the factor β_S arises from a trace involving Dirac matrices, such that

$$\beta_S = -\text{Tr}[(\not{k} + m_1)(\not{k} - \not{P} + m_2)] \quad (2.4)$$

$$= 2P^2 - 2(m_1 + m_2)^2, \quad (2.5)$$

where m_1 and m_2 depend upon temperature. In the frame where $\vec{P} = 0$, and in the case $m_1 = m_2$, we have $\beta_S = 2P_0^2(1 - 4m^2/P_0^2)$. For the scalar case, with $m_1 = m_2$, we find

$$\text{Im } J_S(P^2, T) = \frac{N_c P_0^2}{4\pi} \left(1 - \frac{4m^2}{P_0^2}\right)^{3/2} e^{-\vec{k}^2/\alpha^2} [1 - 2n_1(k)], \quad (2.6)$$

where

$$\vec{k}^2 = \frac{P_0^2}{4} - m^2(T). \quad (2.7)$$

For pseudoscalar mesons, we replace β_S by

$$\beta_P = -\text{Tr}[i\gamma_5(\not{k} + m_1)i\gamma_5(\not{k} - \not{P} + m_2)] \quad (2.8)$$

$$= 2P^2 - 2(m_1 - m_2)^2, \quad (2.9)$$

which for $m_1 = m_2$ is $\beta_P = 2P_0^2$ in the frame where $\vec{P} = 0$. We find, for the π mesons,

$$\text{Im } J_P(P^2, T) = \frac{N_c P_0^2}{4\pi} \left(1 - \frac{4m(T)^2}{P_0^2}\right)^{1/2} e^{-\vec{k}^2/\alpha^2} [1 - 2n_1(k)], \quad (2.10)$$

where $\vec{k}^2 = P_0^2/4 - m_u^2(T)$, as above. Thus, we see that, relative to the scalar case, the phase space factor has an exponent of 1/2 corresponding to a s -wave amplitude. For the scalars, the exponent of the phase-space factor is 3/2, as seen in Eq. (2.6).

For a study of vector mesons we consider

$$\beta_{\mu\nu}^V = \text{Tr}[\gamma_\mu(\not{k} + m_1)\gamma_\nu(\not{k} - \not{P} + m_2)] , \quad (2.11)$$

and calculate

$$g^{\mu\nu}\beta_{\mu\nu}^V = 4[P^2 - m_1^2 - m_2^2 + 4m_1m_2] , \quad (2.12)$$

which, in the equal-mass case, is equal to $4P_0^2 + 8m^2(T)$, when $m_1 = m_2$ and $\vec{P} = 0$. This result will be needed when we calculate the correlator of vector currents in the next section. Note that for the elevated temperatures considered in this work $m_u(T) = m_d(T)$ is quite small, so that $4P_0^2 + 8m_u^2(T)$ can be approximated by $4P_0^2$ when we consider the vector current correlation functions. In that case, we have

$$\text{Im } J_V(P^2, T) \simeq \frac{2}{3} \text{Im } J_P(P^2, T) , \quad (2.13)$$

At this point it is useful to define functions that do not contain the Gaussian regulator:

$$\text{Im } \tilde{J}_P(P^2, T) = \frac{N_c P_0^2}{4\pi} \left(1 - \frac{4m(T)^2}{P_0^2}\right)^{1/2} [1 - 2n_1(k)] , \quad (2.14)$$

and

$$\text{Im } \tilde{J}_V(P^2, T) = \frac{2}{3} \frac{N_c P_0^2}{4\pi} \left(1 - \frac{4m(T)^2}{P_0^2}\right)^{1/2} [1 - 2n_1(k)] . \quad (2.15)$$

For the functions defined in Eq. (2.14) and (2.15) we need to use a twice-subtracted dispersion relation to obtain $\text{Re } \tilde{J}_P(P^2, T)$, or $\text{Re } \tilde{J}_V(P^2, T)$. For example,

$$\begin{aligned} \text{Re } \tilde{J}_P(P^2, T) &= \text{Re } \tilde{J}_P(0, T) + \frac{P^2}{P_0^2} [\text{Re } \tilde{J}_P(P_0^2, T) - \text{Re } \tilde{J}_P(0, T)] + \\ &\quad \frac{P^2(P^2 - P_0^2)}{\pi} \int_{4m^2(T)}^{\tilde{\Lambda}^2} ds \frac{\text{Re } \tilde{J}_P(s, T)}{s(P^2 - s)(P_0^2 - s)} , \end{aligned} \quad (2.16)$$

where $\tilde{\Lambda}^2$ can be quite large since the integral over the imaginary part of the polarization function is now convergent. We may introduce $\tilde{J}_P(P^2, T)$ and $\tilde{J}_V(P^2, T)$ as the complex functions, since we now have both the real and imaginary parts of these functions. We note that the construction of either $\text{Re } J_P(P^2, T)$ or $\text{Re } J_V(P^2, T)$ by means of a dispersion relation does not require a subtraction. We use these functions to define the complex functions $J_P(P^2, T)$ and $J_V(P^2, T)$.

In order to make use of Eq. (2.16) we need to specify $\tilde{J}_P(0)$ and $\tilde{J}_P(P_0^2)$. We found it useful to take $P_0^2 = -1.0$ GeV 2 and to put $\tilde{J}_P(0) = J_P(0)$ and $\tilde{J}_P(P_0^2) = J_P(P_0^2)$. The quantities $\tilde{J}_P(0)$ and $\tilde{J}_P(P_0^2)$ are determined in an analogous function. This procedure in which we fix the behaviors of a function such as $\tilde{J}_V(P^2)$ or $\tilde{J}_V(P^2)$, which may be used when making calculations for large P^2 , is quite analogous to the procedure used in Ref. [14]. In that work we made use of dispersion relations to construct a continuous vector-isovector current correlation function that had the correct perturbative behavior for large $P^2 \rightarrow -\infty$ and also described that low-energy resonance present in the correlator due to the excitation of the ρ meson. In Ref. [14] the NJL model was shown to provide a quite satisfactory description of the low-energy resonant behavior of the vector-isovector correlation function.

III. CALCULATION OF HADRONIC CURRENT CORRELATION FUNCTIONS

In this section we consider the calculation of temperature-dependent hadronic current correlation functions. The general form of the correlator is a transform of a time-ordered product of currents,

$$iC(P^2, T) = \int d^4x e^{iP \cdot x} \ll T(j(x)j(0)) \gg, \quad (3.1)$$

where the double bracket is a reminder that we are considering the finite temperature case.

For the study of pseudoscalar states, we may consider currents of the form $J_{P,i}(x) = \tilde{q}(x)i\gamma_5\lambda^i q(x)$, where, in the case of the π mesons, $i = 1, 2$ and 3 . For the study of scalar-isoscalar mesons, we introduce $j_{S,i}(x) = \tilde{q}(x)\lambda^i q(x)$, where $i = 0$ for the flavor-singlet current and $i = 8$ for the flavor-octet current [7].

In the case of the pseudoscalar-isovector mesons, the correlator may be expressed in terms of the basic vacuum polarization function of the NJL model, $J_P(P^2, T)$ [8, 15, 16]. Thus,

$$C_P(P^2, T) = J_P(P^2, T) \frac{1}{1 - G_P(T)J_P(P^2, T)}, \quad (3.2)$$

where $G_P(T)$ is the coupling constant appropriate for our study of π mesons. We have found $G_P(T) = 13.49$ GeV $^{-2}$ by fitting the pion mass in a calculation made at $T = 0$, with $m_u = m_d = 0.364$ GeV. The result given in Eq. (3.2) is only expected to be useful for small P^2 , since the Gaussian regulator strongly modifies the large P^2 behavior. Therefore, we

suggest that the following form is useful, if we are to consider the larger values of P^2

$$\frac{C_P(P^2, T)}{P^2} = \left[\frac{\tilde{J}_P(P^2, T)}{P^2} \right] \frac{1}{1 - G_P(T)J_P(P^2, T)}. \quad (3.3)$$

(As usual, we put $\vec{P} = 0$.) This form has two important features. At large P_0^2 , $\text{Im} C_P(P_0, T)/P_0^2$ is a constant, since $\text{Im} \tilde{J}_P(P_0^2, T)$ is proportional to P_0^2 . Further, the denominator of Eq. (3.3) goes to 1 for large P_0^2 . On the other hand, at small P_0^2 , the denominator is capable of describing resonant enhancement of the correlation function. As we will see, the results obtained when Eq. (3.3) is used appear quite satisfactory. (We may again refer to Ref. [14], in which a similar approximation is described.)

For a study of the vector-isovector correlators, we introduce conserved vector currents $j_{\mu,i}(x) = \tilde{q}(x)\gamma_\mu\lambda_i q(x)$ with $i=1, 2$ and 3 . In this case we define

$$J_V^{\mu\nu}(P^2, T) = \left(g^{\mu\nu} - \frac{P^\mu P^\nu}{P^2} \right) J_V(P^2, T) \quad (3.4)$$

and

$$C_V^{\mu\nu}(P^2, T) = \left(g^{\mu\nu} - \frac{P^\mu P^\nu}{P^2} \right) C_V(P^2, T), \quad (3.5)$$

taking into account the fact that the current $j_{\mu,i}(x)$ is conserved. We may then use the fact that

$$J_V(P^2, T) = \frac{1}{3} g_{\mu\nu} J_V^{\mu\nu}(P^2, T) \quad (3.6)$$

and

$$\text{Im} J_V(P^2, T) = \frac{2}{3} \left[\frac{P_0^2 + 2m_u^2(T)}{4\pi} \right] \left(1 - \frac{4m_u^2(T)}{P_0^2} \right)^{1/2} e^{-\vec{k}^2/\alpha^2} [1 - 2n_1(k)] \quad (3.7)$$

$$\simeq \frac{2}{3} \text{Im} J_P(P^2, T). \quad (3.8)$$

(See Eq. (3.7) for the specification of $k = |\vec{k}|$.) We then have

$$C_V(P^2, T) = J_V(P^2, T) \frac{1}{1 - G_V(T)J_V(P^2, T)}, \quad (3.9)$$

where we have introduced

$$\text{Im} J_V(P^2, T) = \frac{2}{3} \left[\frac{P_0^2 + 2m_u^2(T)}{4\pi} \right] \left(1 - \frac{4m_u^2(T)}{P_0^2} \right)^{1/2} [1 - 2n_1(k)] \quad (3.10)$$

$$\simeq \frac{2}{3} \text{Im} J_P(P^2, T). \quad (3.11)$$

In the literature, ω is used instead of P_0 [10 -12]. There, the spectral functions

$$\sigma_V(\omega, T) = \frac{1}{\pi} \text{Im} C_V(\omega, T), \quad (3.12)$$

and

$$\sigma_P(\omega, T) = \frac{1}{\pi} \text{Im} C_P(\omega, T), \quad (3.13)$$

are discussed. Since we make use of Eq. (3.6), values of $\sigma_V(\omega, T)$ given in Refs. [10-12] are related to the correlator calculated here by an additional factor of 3/4. Thus, for the sake of comparison to the spectral functions that appear in the literatures [10-12], we replace Eq. (3.12) by

$$\sigma_V(\omega, T) = \frac{3}{4} \cdot \frac{1}{\pi} \text{Im} C_V(\omega, T). \quad (3.14)$$

Inspection of Fig. 1 of Ref. [11] suggests that values of $\sigma_P(\omega, T)$ in that reference are related to our values of $\text{Im} C_P(\omega, T)$ by the relation

$$\sigma_P(\omega, T) = \frac{1}{2} \cdot \frac{1}{\pi} \text{Im} C_P(\omega, T). \quad (3.15)$$

We will use Eqs. (3.14) and (3.15) when making comparison to the results given in Refs. [10-12].

In addition to providing values of $\sigma_V(\omega, T)/\omega^2$ and $\sigma_P(\omega, T)/\omega^2$ the τ -dependent hadronic correlators $G_P(\tau, T)$ and $G_V(\tau, T)$ were introduced [10-12], with

$$G(\tau, T) = \int_0^\infty d\omega \sigma(\omega, T) K(\omega, \tau, T). \quad (3.16)$$

Here,

$$K(\omega, \tau, T) = \frac{\cosh[\omega(\tau - \frac{1}{2T})]}{\sinh(\frac{\omega}{2T})}. \quad (3.17)$$

We will present results of our calculations of $G_P(\tau, T)$ and $G_V(\tau, T)$ in Sections IV and V, respectively. We will also present the values obtained for $\text{Im} C_P(P_0, T)/P_0^2$ and $\text{Im} C_V(P_0, T)/P_0^2$ for various values of T/T_c in Sections IV and V.

IV. CORRELATION FUNCTIONS FOR PSEUDOSCALAR-ISOVECTOR CURRENTS - NUMERICAL RESULTS

In Fig. 3 we show $\text{Im} C_P(P_0, T)/P_0^2$ for $T/T_c = 1.5$, and for model 1, as a solid line. The dashed line represents the result at $T/T_c = 1.5$, if we put $G_P(T) = 0$. The results for

a broader range of temperatures are shown in Fig. 4. The value for $T/T_c = 1.5$, shown as a dashed line in Fig. 4, may be compared to the results shown in Fig. 1 of Ref. [11] which exhibits $\sigma_P(\omega, T)/\omega^2$ as a dotted line with a maximum value of about 0.17. We may compare that result with the maximum of the dashed curve of our Fig. 4. Using Eq. (3.15) and dividing our result by 2π , we have a value of 0.065, which is smaller than the value 0.17 obtained from Ref. [11]. In Fig. 5, we show the results for model 2 at the same values of T/T_c used to construct Fig. 4. Performing the same comparison as that made for Fig. 4 at $T/T_c = 1.5$, we find a maximum value of 0.09, which is closer to the 0.17 value of Ref. [11] than the 0.065 value obtained from model 1. If we put $T_c = 150$ MeV, the peak at $T/T_c = 1.5$ in Fig. 5 is at about 500 MeV, which the corresponding peak in Fig. 1 of Ref. [11] is at about 1.0 GeV. To obtain some support for our value of 500 MeV, rather than the 1 GeV value of Ref. [11], we may refer to Fig. 6.7 on page 332 of Ref. [15]. There, the values are given for the temperature-dependent masses of the σ and π mesons calculated in the NJL model without confinement. If we take $T_c = 150$ MeV, we have $T = 225$ MeV at $T/T_c = 1.5$. From Fig. 6.7 of Ref. [15], we observe that the π mass is quite close to 500 MeV, if we make a modest extrapolation of the results given in the figure from 200 MeV to 225 MeV. That suggests that, our result of 500 MeV for the peak of the pseudoscalar-isovector correlation function at $T/T_c = 1.5$ is to be preferred over the value of 1 GeV obtained from the results presented in Ref. [11].

From a inspection of Fig. 2 of Ref. [12], we see that the lattice results have quite large errors, such that the magnitude of the peaks and the positions of their maxima could be uncertain to within a factor of 2. That feature may explain why the resonant structure seen for $T/T_c = 3.0$ in Ref. [11] and [12] is not seen in our Fig. 4 and 5. Again referring to Fig. 2 of Ref. [12], we see that, when the errors are taken into account, it is possible that our result at $T/T_c = 3.0$ is compatible with that given in Ref. [11].

In Fig. 6 we show, as a dashed line, values of $\text{Im } C_P(P_0, T)/P_0^2$ at $T/T_c = 5.88$ obtained using a constant value of $G_P(T) = 13.49$ GeV $^{-2}$. The solid line is the result for model 1(or model 2) at $T/T_c = 5.88$, in which case $G_P(T) = 0$ for both models. Since we have argued that for $T/T_c \sim 6$ the quark-gluon plasma should be a weakly interacting system, the use of a constant value for $G_P(T)$ appears to be unacceptable. We present this result to support our argument that the coupling parameters of the chiral Lagrangian model should be made temperature dependent to be consistent with QCD thermodynamics.

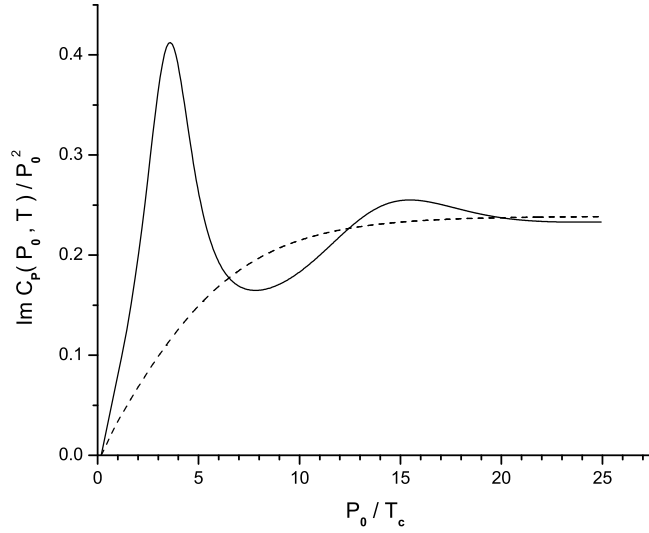


FIG. 3: Values of $\text{Im } C_P(P_0, T)/P_0^2$ are shown at $T/T_c = 1.5$ for model 1, where $G_P(T) = G_P[1 - 0.17(T/T_c)]$ (solid line). The dashed line represents the result obtained when $T/T_c = 1.5$ and $G_P(T) = 0$. (Here, the dashed line represents the values of $\text{Im } \tilde{J}_P(P_0, T)/P_0^2$ for $T/T_c = 1.5$.)

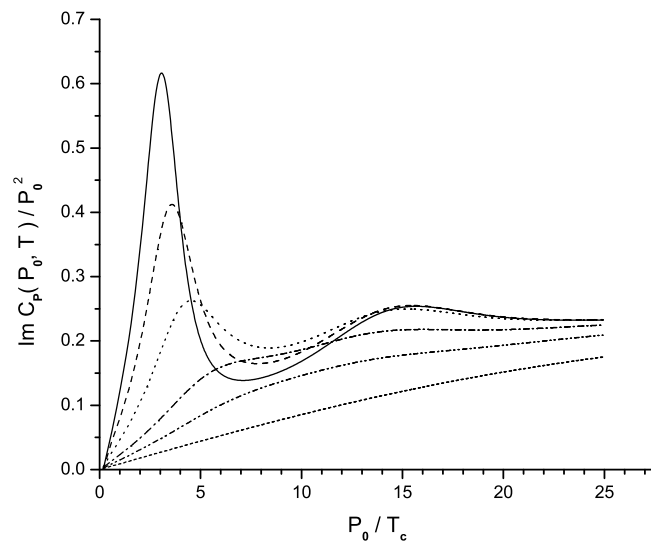


FIG. 4: Values of $\text{Im } C_P(P_0, T)/P_0^2$ are shown for model 1 and for various temperatures: $T/T_c = 1.2$ [solid line], $T/T_c = 1.5$ [dashed line], $T/T_c = 2.0$ [dotted line], $T/T_c = 3.0$ [dashed-dotted line], $T/T_c = 4.0$ [dashed-double dotted line], $T/T_c = 5.88$ [short-dashed line].

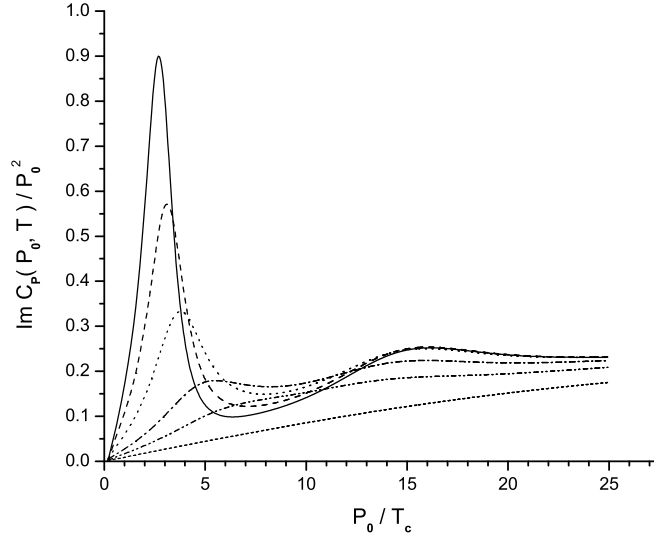


FIG. 5: Values of $\text{Im } C_P(P_0, T)/P_0^2$ are shown at for various temperatures for model 2, with $G_P(T) = G_P[1 - 0.0289 (T/T_c)^2]$. (See the caption to Fig. 2.)

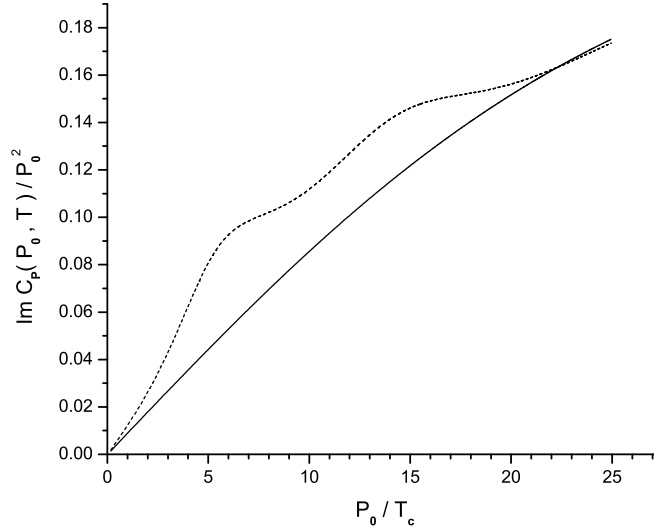


FIG. 6: Values of $\text{Im } C_P(P_0, T)/P_0^2$ are shown for $T/T_c = 5.88$. The dashed line represents the result when $G_P(T) = G_P = 13.49 \text{ GeV}^{-2}$. The solid line is the result for $G_P(T) = 0$, which is characteristic of models 1 and 2, when $T/T_c = 5.88$. (The solid line, therefore, represents the values of $\text{Im } \tilde{J}_P(P_0, T)/P_0^2$ for $T/T_c = 5.88$.)

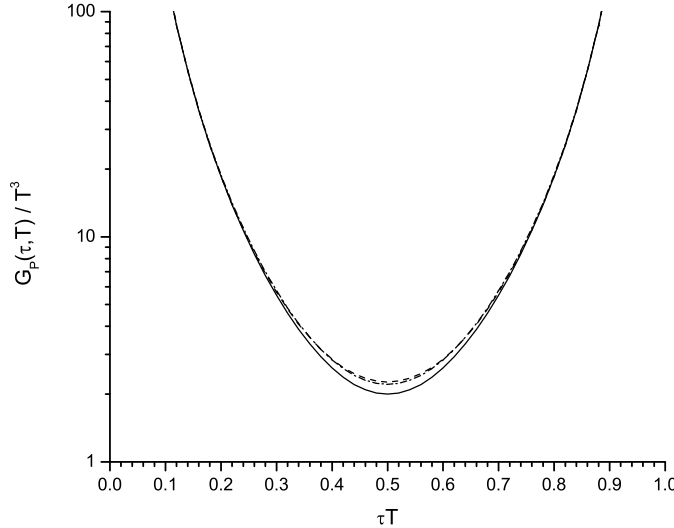


FIG. 7: Values of $G_P(\tau, T)/T^3$ are shown for $T/T_c = 1.5$ [dashed line], $T/T_c = 3.0$ [dashed-dotted line], $T/T_c = 5.88$ [solid line]. These results were calculated with model 1.

In Fig. 7 we show values of $G_P(\tau, T)/T^3$ for $T/T_c = 1.5$ [dashed line], $T/T_c = 3.0$ [dashed-dotted line] and $T/T_c = 5.88$ [solid line]. These results maybe compared to those shown in Fig. 1 of Ref. [11], which also exhibits the values for $T \rightarrow \infty$. In Fig. 1 of Ref. [11] we see a marked difference in the behavior of $G_P(\tau, T)/T^3$ and $G_V(\tau, T)/T^3$. (We will present some discussion of this matter in Sec. V.)

V. CORRELATION FUNCTIONS FOR VECTOR-ISOVECTOR CURRENTS - NUMERICAL RESULTS

In Fig. 8 we show the values of $\text{Im} C_V(P_0, T)/P_0^2$ for model 1 and for $T/T_c = 1.5$, as a solid line. The result for $T/T_c = 1.5$ and $G_V(T) = 0$ is represented by the dashed line. [See Fig. 3]. In Fig. 9 we show values of $\text{Im} C_V(P_0, T)/P_0^2$ for various values of T/T_c and for model 1. Corresponding results for model 2 are given in Fig. 10. In Figs. 9 and 10, we do not see the resonances reported at $T/T_c = 3.0$ in Refs. [10-12].

In Fig. 11 we show, as a dashed line, values for $T/T_c = 5.88$ of $\text{Im} C_V(P_0, T)/P_0^2$, which were calculated with a constant value of $G_V(T) = 11.46 \text{ GeV}^{-2}$. The solid line represents the results for $G_V(T) = 0$, which is characteristic of models 1 and 2 when $T/T_c = 5.88$. The comments made with respect to Fig. 6 are also applicable here.

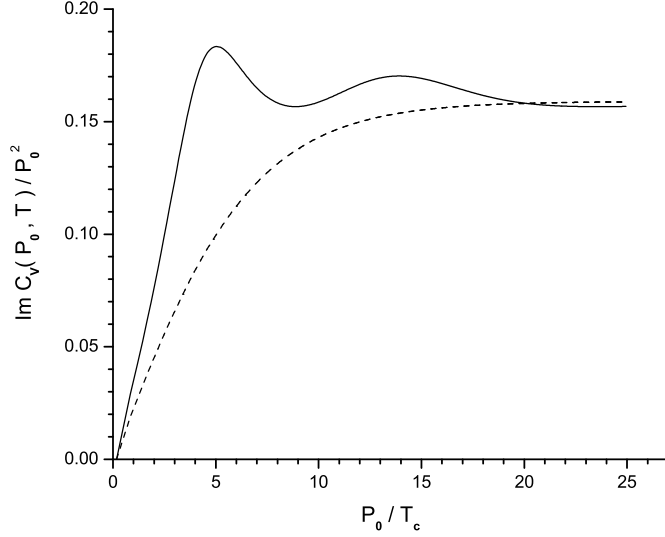


FIG. 8: Values of $\text{Im } C_V(P_0, T)/P_0^2$ are shown for $T/T_c = 1.5$. (See the caption of Fig. 3.)

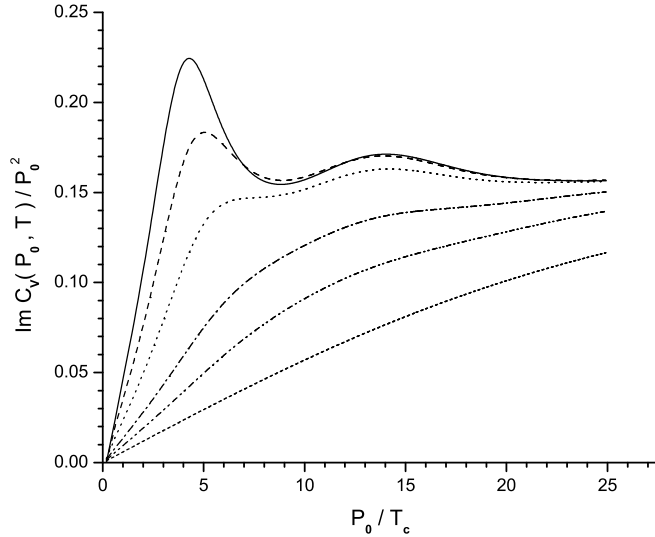


FIG. 9: Values of $\text{Im } C_V(P_0, T)/P_0^2$ are shown for model 1 and for various temperatures. (See the caption of Fig. 4.)

In Fig. 12 we show values of $G_V(\tau, T)/T^3$ for $T/T_c = 1.5$ [dashed line], $T/T_c = 3.0$ [dash-dotted line] and $T/T_c = 5.88$ [solid line]. These results are obtained with model 1, and may be compared to those shown in Fig. 7, where we see generally similar behavior. That is in strong contrast to the results shown in Ref. [11], where $G_V(\tau, T)/T^3$ and $G_P(\tau, T)/T^3$ shown quite different behavior, with the result for the vector correlator close to the $T \rightarrow \infty$

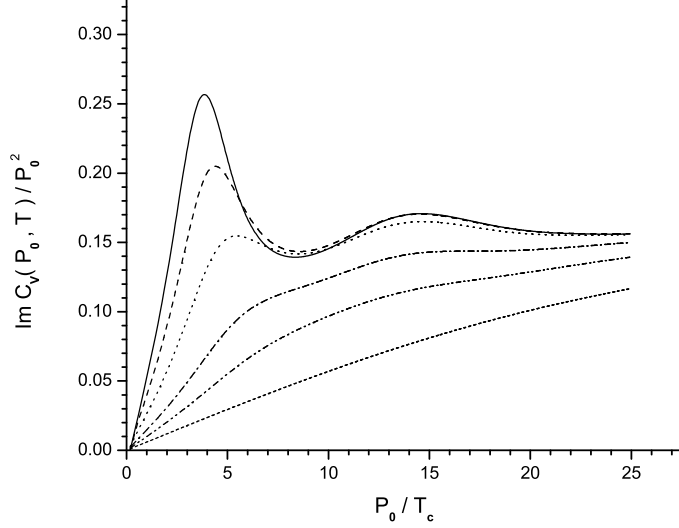


FIG. 10: Values of $\text{Im } C_V(P_0, T) / P_0^2$ are shown for model 2 and for various temperatures. (See the caption of Fig. 4.)

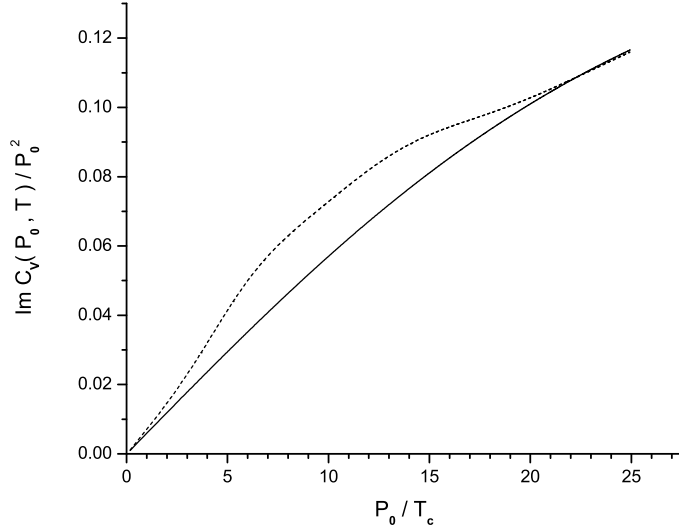


FIG. 11: Values of $\text{Im } C_V(P_0, T) / P_0^2$ are shown for $T/T_c = 5.88$. (See the caption of Fig. 6.)

result at $T/T_c = 1.5$ and $T/T_c = 3.0$. This suggests that the value of $G_V = 11.46 \text{ GeV}^{-2}$ that we have used in this work may be too large, or that the temperature dependence of $G_V(T)$ is such as to yield smaller values than those obtained in this work for model 1 or model 2. Therefore, in Fig. 13 we show $\text{Im } C_V(P_0, T) / P_0^2$ for $T = 1.5 T_c$, for model 1, with $G_V = 11.46 \text{ GeV}^{-2}$ [solid line], $G_V = 8.00 \text{ GeV}^{-2}$ [dashed line], $G_V = 4.0 \text{ GeV}^{-2}$ [dotted line]

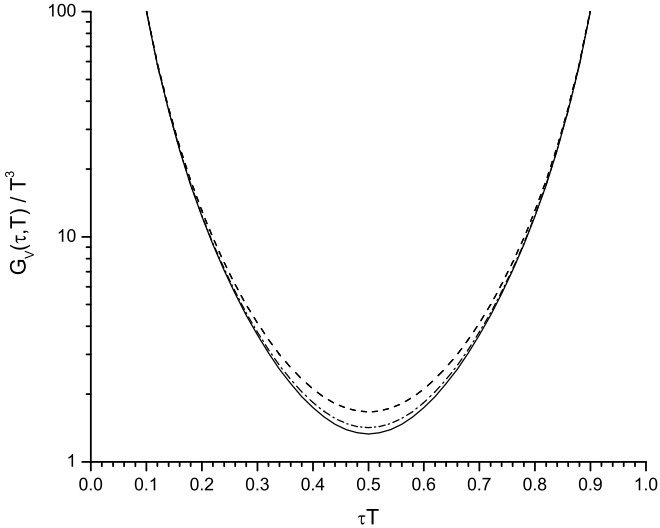


FIG. 12: Values of $G_V(\tau, T)/T^3$ are shown for $T/T_c = 1.5$ [dashed line], $T/T_c = 3.0$ [dashed-dotted line], $T/T_c = 5.88$ [solid line]. These results were calculated with model 1.

and $G_V = 0.0 \text{ GeV}^{-2}$ [dot-dashed line]. It would be of interest to consider the results of Ref. [11] for the Euclidean-space correlator to be correct and to then determine $G_V(T)$ so that we fit the values of $G_V(\tau, T)/T^3$ obtained in the lattice calculations. We defer such a project to a future work.

VI. DISCUSSION

It is difficult to make a definitive comparison of our results and the results obtained for the spectral functions in the lattice simulations, since those results are accompanied by large errors. Also, it is somewhat difficult to understand why the different behavior seen for $G_V(\tau, T)/T^3$ and $G_P(\tau, T)/T^3$ in Ref. [11], leads to values for $\sigma_P(\omega, T)/\omega^3$ and $\sigma_V(\omega, T)/\omega^3$ that are rather similar [10-12]. As noted earlier, we do not see the resonant behavior at $T/T_c = 3.0$ suggested by the lattice simulation. On the other hand, the chiral Lagrangian model provides a systematic study, which may provide some guidance for further studies of lattice QCD. This may be particularly important in the light of the comments made in Ref. [11]:

”The reconstruction of $\sigma_H(\omega, T)$ and in particular the determination of its low

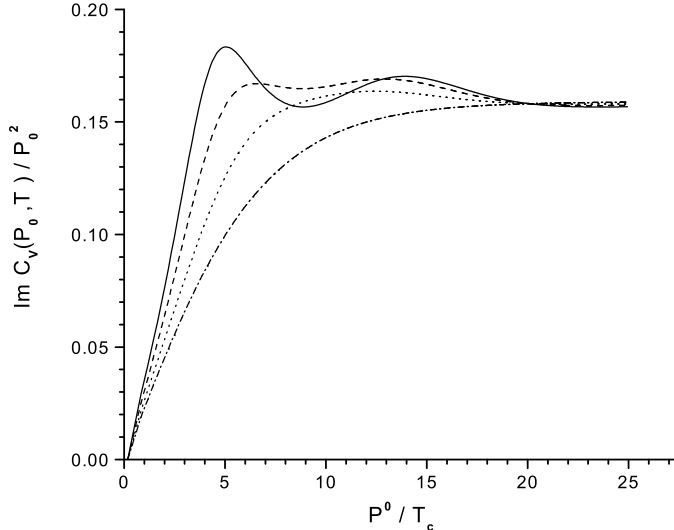


FIG. 13: Values of $\text{Im } C_V(P_0, T) / P_0^2$ are shown for $T/T_c = 1.5$ with $G_V = 11.46 \text{ GeV}^{-2}$ [solid line], $G_V = 8.00 \text{ GeV}^{-2}$ [dashed line], $G_V = 4.00 \text{ GeV}^{-2}$ [dotted line] and $G_V = 0.0 \text{ GeV}^{-2}$ [dot-dashed line]. Here, we used model 1.

energy structure thus is difficult at non-zero temperature. Additional complications arise in lattice calculations which necessarily are performed on lattices with finite number of points (N_τ) in Euclidean time. The correlation functions $G_H(\tau, T)$ can thus be calculated only at finite set of Euclidean times $\tau T = k/N_\tau$, with $k = 0, \dots, N_\tau - 1$. In order to reconstruct the spectral functions from this limited set of information it is necessary to include in the statistical analysis of numerical results also prior information on the structure of $G_H(\tau, T)$ as well as assumptions about the likelihood of a certain spectral function $\sigma_H(\omega, T)$. It has been suggested to provide this additional information through the application of the Maximum Entropy Method (MEM) [17, 18], which has been applied successfully to many other ill-conditioned problems in physics . . .”

[1] For reviews, see K. Rajagopal and F. Wilczek, in *At the Frontier of Particle Physics/Handbook of QCD*, M. Shifman ed. (World Scientific, Singapore 2001); M. Alford, *Annu. Rev. Nucl. Part. Sci.* **51**, 131 (2001).

[2] Z. Fodor and S. D. Katz, hep-lat/0204029; *Nucl. Phys. B (Proc. Suppl.)* **106**, 441 (2002) [hep-lat/0106002]; *Phys. Lett. B* **534**, 87 (2002).

[3] Hu Li and C. M. Shakin, *Phys. Rev. D* **66**, 074016 (2002).

[4] Bing He, Hu Li, C. M. Shakin, and Qing Sun, hep-ph/0211318.

[5] M. Le Bellac, *Thermal Field Theory* (Cambridge Univ. Press, Cambridge, 1996)-See Fig. 1.3.

[6] Hu Li and C. M. Shakin, hep-ph/0209136.

[7] Hu Li and C. M. Shakin, hep-ph/0209258.

[8] S. P. Klevansky, *Rev. Mod. Phys.* **64**, 649 (1992). [See Eq.(5.38) of this reference.]

[9] Bing He, Hu Li, C. M. Shakin, and Qing Sun, hep-ph/0203010.

[10] I. Wetzorke, F. Karsch, E.Laermann, P. Petreczky, and S. Stickan, hep-lat/0110132.

[11] F. Karsch, S. Datta, E.Laermann, P. Petreczky, and S. Stickan, and I. Wetzorke, hep-ph/0209028.

[12] F. Karsch, E.Laermann, P. Petreczky, S. Stickan, and I. Wetzorke, *Phys. Lett. B* **530**, 147 (2002).

[13] R. L. Kobes and G. W. Semenoff, *Nucl. Phys. B* **260**, 714 (1985).

[14] C. M. Shakin, Wei-Dong Sun, and J. Szweda, *Ann of Phys. (NY)* **241**, 37 (1995).

[15] T. Hatsuda and T. Kunihiro, *Phys. Rep.* **247**, 221 (1994).

[16] V. Vogl and W. Weise, *Prog. Part. Nucl. Phys.* **27**, 195 (1991).

[17] M. Asakawa, T. Hatsuda and Y. Nakahara, *Prog. Part. Nucl. Phys.* **46**, 459 (2001)

[18] Y. Nakahara, M. Asakawa and T. Hatsuda, *Phys. Rev. D* **60** 091503 (1999).